

## Effect of permeability on foam-model parameters

### An integrated approach from core-flood experiments through to foam diversion calculations

Kapetas, L.; Vincent Bonnieu, S.; Farajzadeh, R.; Eftekhari, A. A.; Shafian, S. R. Mohd; Bahrim, R. Z. Kamarul; Rossen, W. R.

#### DOI

[10.1016/j.colsurfa.2017.06.060](https://doi.org/10.1016/j.colsurfa.2017.06.060)

#### Publication date

2017

#### Document Version

Final published version

#### Published in

Colloids and Surfaces A: Physicochemical and Engineering Aspects

#### Citation (APA)

Kapetas, L., Vincent Bonnieu, S., Farajzadeh, R., Eftekhari, A. A., Shafian, S. R. M., Bahrim, R. Z. K., & Rossen, W. R. (2017). Effect of permeability on foam-model parameters: An integrated approach from core-flood experiments through to foam diversion calculations. *Colloids and Surfaces A: Physicochemical and Engineering Aspects*, 530, 172-180. <https://doi.org/10.1016/j.colsurfa.2017.06.060>

#### Important note

To cite this publication, please use the final published version (if applicable).  
Please check the document version above.

#### Copyright

Other than for strictly personal use, it is not permitted to download, forward or distribute the text or part of it, without the consent of the author(s) and/or copyright holder(s), unless the work is under an open content license such as Creative Commons.

#### Takedown policy

Please contact us and provide details if you believe this document breaches copyrights.  
We will remove access to the work immediately and investigate your claim.



ELSEVIER

Contents lists available at ScienceDirect

Colloids and Surfaces A

journal homepage: [www.elsevier.com/locate/colsurfa](http://www.elsevier.com/locate/colsurfa)

## Effect of permeability on foam-model parameters: An integrated approach from core-flood experiments through to foam diversion calculations



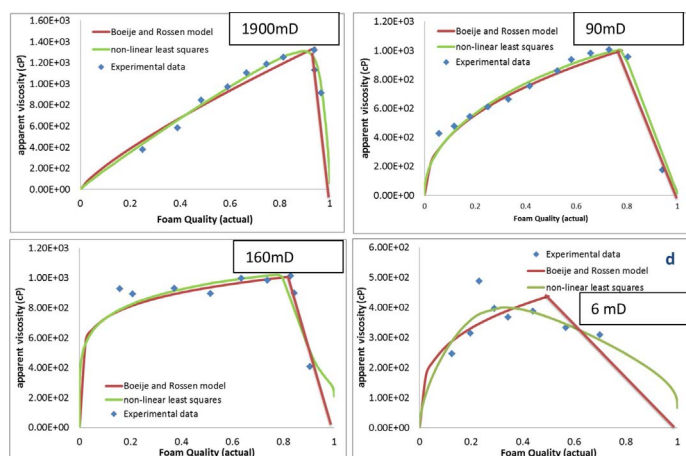
L. Kapetas<sup>a</sup>, S. Vincent Bonnieu<sup>a,b,\*</sup>, R. Farajzadeh<sup>a,b</sup>, A.A. Eftekhari<sup>a</sup>, S.R. Mohd Shafian<sup>c</sup>, R.Z. Kamarul Bahrin<sup>c</sup>, W.R. Rossen<sup>a</sup>

<sup>a</sup> Department of Geoscience and Engineering, Delft University of Technology, Netherlands

<sup>b</sup> Shell Global Solutions International BV, Netherlands

<sup>c</sup> PETRONAS Research Sdn Bhd, Malaysia

### GRAPHICAL ABSTRACT



### ARTICLE INFO

#### Keywords:

Foam  
Flooding  
Oil recovery  
Flow in porous media  
Permeability  
Simulation

### ABSTRACT

We present a set of steady-state foam-flood experimental data for four sandstones with different permeabilities, ranging between 6 and 1900 mD, and with similar porosity. We derive permeability-dependent foam parameters with two modelling approaches, those of Boeije and Rossen (2015a) and a non-linear least-square minimization approach (Eftekhari et al., 2015). The two approaches can yield significantly different foam parameters. Thus, we critically assess their ability in deriving reliable foam parameter estimates. In particular, the way the two approaches treat shear-thinning foam behaviour and foam coalescence is discussed. The foam parameter set acquired from the latter approach is further used as input in foam diversion calculations: this serves to evaluate mobility predictions in non-communicating reservoir layers. This study aims to provide a framework to integrate experimental work, modelling and simple qualitative diversion calculations to provide a background for the upscaling of foam studies, with particular focus on heterogeneous systems.

\* Corresponding author.

E-mail address: [s.vincentbonnieu@shell.com](mailto:s.vincentbonnieu@shell.com) (S. Vincent Bonnieu).

<http://dx.doi.org/10.1016/j.colsurfa.2017.06.060>

Received 10 October 2016; Received in revised form 21 June 2017; Accepted 21 June 2017

Available online 08 July 2017

0927-7757/ © 2017 Elsevier B.V. All rights reserved.

## 1. Introduction

Foam is a dispersion of gas bubbles in a continuous liquid medium where bubbles are separated by thin films called lamellae. Foam can be used in enhanced oil recovery (EOR) to control gas mobility and deal with phenomena such as gas gravity override, viscous fingering and preferential channeling due to reservoir heterogeneity [1,2]. To date, relatively few field or pilot applications have been conducted. This is partly due to the incomplete understanding of how foam will behave in the field. Several studies aim at reducing uncertainty in foam processes by studying chemical and physical factors. The effect of liquid and gas composition [3–5], the effect of oil composition and saturation [6–10], and the effects of miscibility, pressure or temperature [11–13] have been studied in laboratory-scale core-floods.

Foam models are divided into two main categories: Population Balance (PB) models aim to take into account the complex dynamics which are involved in foam-generation and –destruction processes. Their goal is to capture the influence of such processes by describing the dynamic evolution of foam texture, or bubble size [14–20,47]. Changing gas mobility is represented as a function of foam texture. Dynamic population-balance models can be restricted to assume local equilibrium between processes of creation and destruction of foam lamellae [20–23]; in this case, foam obtains its steady-state texture instantaneously. This simplification implies also that gas mobility reduction is reached instantly. Other models reflect the effects of foam texture implicitly through a gas mobility-reduction factor [24–28]. These models, which we call “implicit texture” (IT) models here, all assume local equilibrium. In most published model applications, local equilibrium is an accurate approximation [18,20], with the exception of the entrance region where foam is generated [21,18,20,29] and at shock fronts [30,20]. In cases where foam generation need to be explicitly modeled, a population-balance approach is essential [15,23,31,32].

Foam core-floods are used to fit foam model parameters in two main ways [33]: (i) Dynamic Surfactant Alternating Gas (SAG) injection floods where gas is injected into a surfactant-saturated core. Transient SAG flood pressure gradient data over time are then fitted to derive foam-model parameters. (ii) Co-injection experiments where surfactant solution is injected together with gas until steady state is reached for different foam qualities, i.e. different injected volume fractions of gas. In this case, steady-state pressure-gradient data are obtained as a function of foam quality and subsequently fitted to derive foam-parameters [33–35]. Such experimental data, also known as foam scans, typically reflect foam in both the so-called “low-quality” and “high-quality” regimes: in the former regime the pressure drop is nearly independent of liquid velocity, and in the latter the pressure drop is nearly independent of gas velocity [36,37].

This work deals only with the modelling of co-injection steady-state foam data and the derivation of IT modelling parameters based on them. The reason for this is that laboratory SAG floods can introduce uncertainties due to slow foam-generation dynamics in the laboratory [38]. This study fits steady-state pressure-gradient data in both the low- and high-quality regimes. As discussed in Boeije and Rossen [34,46], fitting data only to high-quality data is a more accurate approach if one’s ultimate purpose is to simulate a field SAG flood application. However, generating such data requires extremely precise measurements, which are hard to obtain (or to verify their precision). Available approaches for fitting IT parameters to co-injection steady-state pressure gradient data include those of Boeije and Rossen [34,46], Ma et al. [33] and the non-linear least-square fitting approach of Eftekhari et al. [35] (see also [12]). The derived parameters can represent the effect of water saturation and shear-thinning foam rheology in a simulation. The last two approaches bear significant similarities; in this work the approaches of Boeije and Rossen [34,46] and Eftekhari et al. [35] are discussed in detail (see Methods and Results sections). Up-scaled reservoir simulations use the IT parameters defined through the

experimental data-fitting to predict the performance of foam in field-scale studies. The most commonly used foam simulation tools are STARS Computer Modelling Group, 2015, UTCHEM [28] and ECLIPSE [39].

This work investigates the effect of permeability on foam behaviour. The results of this study have been presented in the conference proceeding of EAGE conference in 2015 [12,13]. For this, co-injection foam-flood experiments are carried out using sandstone cores of different permeabilities. The results are fitted to derive foam-model parameters. These are subsequently used for diversion calculations for a heterogeneous formation with non-communicating layers to qualitatively evaluate conformance control in such settings. The effect of oil on foam is important and complex [40]. Correctly modelling foam without oil is a necessary first step toward representing foam with oil. Therefore, for simplicity, this paper focuses on foam behaviour in the absence of oil.

## 2. Methods

### 2.1. Experiments

Core-flood experiments were carried out using four different sandstone cores (Kocurek Industries Inc.; Austin, TX): Bentheimer, Berea, Sister Berea, and Bandera Gray. Table 1 reports the absolute permeability and porosity values for the cores ( $D = 2.54$  cm,  $L = 3.81$  cm) used to measure relative-permeability curves. The specific sandstones were selected due to their homogeneous characterization, their similarity in porosity and widely differing permeability. The cores in the foam experiments were 38 cm long with a diameter of 3.8 cm. The core-flood experimental setup is shown schematically in Fig. 1. The procedure is as follows. A confining pressure is applied to the core for the duration of the experiment. Pressure taps allow pressure-drop measurements in 4 different sections of the core: the two sections close to the inlet and the outlet are 5.5 cm long, and the two middle sections are each 13.5 cm long. The reported pressure drops in this work are for the “ $dP_2$ ” section (third section in the direction of flow), to minimize entrance-region and capillary end effects. The PEEK core holder is placed vertically and the experiments took place at room temperature. Injection was from the bottom of the core. A back-pressure regulator controlled the downstream pressure to a nearly constant value of  $20 \pm 0.3$  bar.

In the case of the least-permeable sandstone, Bandera Gray, the experiment was conducted in a shorter core, 17 cm long, to avoid excessive injection pressure. The reported pressure drop was for the middle 6.5 cm section. The other features of the setup were as in Fig. 1. This setup was used and described previously in Kapetas et al. [12]. The surfactant formulation was 1 wt% C14-16 AOS surfactant (STEPAN), in 1 wt% NaCl brine.

The protocol before initiating the foam experiments consisted of the following steps [12]: (i) connection and leakage testing at 20 bar with Helium, (ii) injection of several pore volumes (PV) of  $CO_2$  to displace air inside the core, (iii) displacement of  $CO_2$  with 6 PV brine at 20 bar back-pressure, and (iv) flooding with 5 PV of surfactant solution to

**Table 1**  
Absolute and relative-permeability (Corey) parameters see Eqs. (3) and (4).

Sandstone	Bentheimer	Berea	Sister Berea	Bandera Gray
Brine Perm(mD)	773	137	116	13
Porosity	0.24	0.20	0.21	0.23
$S_{wc}$	0.25	0.23	0.25	0.46
$S_{rg}$	0.20	0.12	0.25	0.00
$n_w$	2.86	4.09	5.25	3.56
$n_g$	0.70	1.97	1.22	2.43
$k_{rw}^o$	0.39	0.39	0.14	1.00
$k_{rg}^o$	0.59	0.99	0.47	0.73

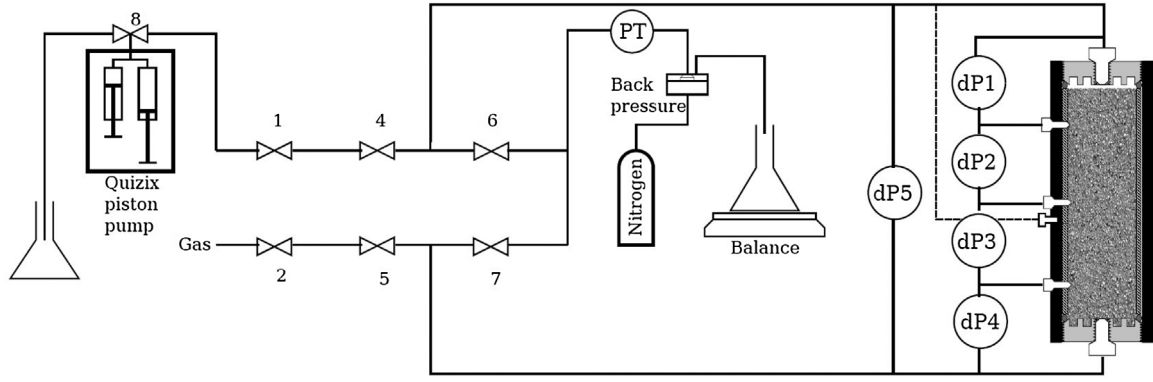


Fig. 1. Core-flooding experimental setup. Elements include valves, injection points, core inside core-holder, back-pressure regulator, and effluent collection and weighing.

ensure that adsorption of surfactant on the sandstone was satisfied. Permeability was measured during the last two steps and co-injection of surfactant solution and gas was then initiated. The surface tension of the surfactant solution was 28 mN/m at 20 °C, measured with the De Noüy ring method. The surfactant viscosity was 1.08 mPa s.

Foam quality and total superficial velocity were controlled by varying the rates of injection of N<sub>2</sub> gas and AOS solution to maintain the desired values for the average pressure in section “dP<sub>2</sub>”. Steady state was considered to be established at a new foam quality when the recorded pressure drop reached a constant value and varied by less than  $\pm 0.2$  bar over a period of 2 h. A mass balance based on the mass of liquid injected and the effluent was used to confirm a stable saturation once steady state was attained. Gas superficial velocity was calculated at the average pressure in section dP<sub>2</sub> by applying two corrections [12]: (i) with respect to the injection pressure set on the Mass Flow Controller (i.e., an adjustment for use of the mass flow controller at a different pressure from its calibration), (ii) with respect to gas compressibility. The latter calculation was performed by applying the Jacobsen-Stewart equation of state [41].

Pressure-drop measurements allow the calculation of the apparent viscosity [33]:

$$\mu_{app}(S_w) \equiv \frac{k \nabla P}{u} \quad (1)$$

where  $k$  is absolute permeability,  $\nabla P$  the magnitude of pressure gradient and  $u$  total superficial velocity. The values of apparent viscosity at different foam qualities constitute a foam scan.

Relative permeability for N<sub>2</sub> gas and (surfactant free) brine solution was measured with the unsteady-displacement method [42] which allowed the estimation of the Corey parameters, water saturation at residual gas conditions  $S_{gr}$ , and connate water saturation,  $S_{wc}$  (see Eqs. (3) and (4) below). The parameter values for the four sandstone cores are reported in Table 1.

## 2.2. Modeling

The inverse mobility reduction factor, FM, represents the factor by which gas mobility is reduced due to the presence of foam, relative to gas mobility at the same water saturation in the absence of foam. Foam apparent viscosity is related to FM by Eq. (2):

$$\mu_{app}(S_w) = \frac{1}{\frac{k_{rw}(S_w)}{\mu_w} + \frac{FM \times k_{rg}(S_w)}{\mu_g}} \quad (2)$$

where water and foam-free relative permeabilities are described by the Corey-type equations:

$$k_{rg}(S_w) = k_{rg}^0 \left( \frac{1 - S_w - S_{gr}}{1 - S_{wc} - S_{gr}} \right)^{n_g} \quad (3)$$

$$k_{rw}(S_w) = k_{rw}^0 \left( \frac{S_w - S_{wc}}{1 - S_{wc} - S_{gr}} \right)^{n_w} \quad (4)$$

where  $k_{rw}$  is the water relative permeability,  $k_{rw}^0$  the end-point water relative permeability,  $k_{rg}$  the gas relative permeability in the absence of foam,  $k_{rg}^0$  the end-point gas relative permeability in absence of foam and  $n_w$  and  $n_g$  the exponents in the relative-permeability curves. If  $S_w \leq S_{wc}$  then  $k_{rw} = 0$  and if  $S_w \geq 1 - S_{gr}$  then  $k_{rg} = 0$ . In the presence of surfactant and absence of oil the STARS foam model [43] relates FM to two functions of water saturation and capillary number:

$$FM = \frac{1}{1 + fmmob \times F_2 \times F_5} \quad (5)$$

where  $fmmob$  is the reference mobility reduction factor,  $F_2$  is a function of water saturation and describes coalescence, and  $F_5$  is a shear-thinning function. In its definition, the STARS model assumes that the functions  $F_2$  and  $F_5$  can only increase the value of FM. Thus, they each cannot exceed a value of 1. The functions  $F_2$  and  $F_5$  are shown in Eqs. (6) and (7) respectively:

$$F_2 = 0.5 + \frac{\arctan(epdry(S_w - fmdry))}{\pi} \quad (6)$$

$$F_5 = \begin{cases} \left( \frac{fmcap}{N_{ca}} \right)^{epcap} & N_{ca} \geq fmcap \\ 1 & N_{ca} < fmcap \end{cases} \quad (7)$$

where the capillary number,  $N_{ca}$ , represents the balance of viscous forces against surface tension,  $\sigma_{wg}$  (Eq. (8)):

$$N_{ca} = \frac{\mu_{app} \cdot u}{\sigma_{wg}} = \frac{k \cdot \nabla P}{\sigma_{wg}} \quad (8)$$

Thus the foam model we use contains five parameters:  $fmmob$ ,  $epdry$ ,  $fmdry$ ,  $fmcap$  and  $epcap$ . Parameter  $epdry$  controls the abruptness of the foam collapse as a function of water saturation. Small values give a gradual transition between the two regimes, while larger values yield a sharper, albeit still continuous, transition. If the transition between regimes is abrupt, the parameter  $fmdry$  is equal to  $S_w^*$ , the water saturation at the limiting capillary pressure  $P_c^*$ , i.e. the water saturation at which foam collapses [44,45]. Parameter  $epcap$  controls the significance of shear-thinning; the larger it is, the stronger the shearing thinning behaviour effect becomes. A value  $epcap = 0$  represents Newtonian behaviour. As mentioned, the STARS model caps the value of function  $F_5$  to a maximum of 1. Thus, the value of  $fmcap$  should be set equal to the lowest capillary number expected in the simulations. Below this value of capillary number (i.e. below  $fmcap$ ) shear-thinning behaviour is not represented. Thus  $fmcap$  is not a foam parameter per se, leaving four independent parameters,  $fmmob$ ,  $fmdry$ ,  $epdry$ , and  $epcap$ .

Fitting of the foam scans to obtain foam parameters was carried out with two techniques:

- (i) the approach of Boeije and Rossen [34,46], which is suitable for simulations of foam processes at finite water fraction. This approach is simple and direct since parameter estimation can be performed with simple calculations. The method assumes a large value of  $epdry$ , i.e. an abrupt transition between low and high quality regimes.
- (ii) a non-linear least-square minimization approach [35]. This was developed in MATLAB and it simultaneously computes all four foam parameters by minimizing the sum of squared errors. For this, an initial guess and an allowed range is required for each parameter. Equal weights were assigned to all experimental data during fitting.

In the modelling section below, function  $F_5$  is sometimes allowed to exceed a value of 1, in violation of Eq. (4). We choose not to set this cap on  $F_5$  as assumed in STARS simulations in order to demonstrate the effect of shear thinning in scenarios where the studied velocities and pressure gradients (or equivalently capillary numbers) are lower than those observed in the lab, i.e. than the experimental pressure gradient data from which the model parameters were obtained.

### 3. Results

#### 3.1. Experiments

Fig. 2 presents the experimental data for the foam scans of the four sandstone cores. The model fits appearing in the graphs are discussed later. As reported in Fig. 2, the permeability values for the sandstone cores under study vary somewhat from the values measured in the relative-permeability measurements, since the samples were different. In a hypothetical field application, with a layered reservoir, for instance, layers would be roughly the same pressure gradient in each of the layers, not the same superficial velocity. In order to compare these experiments, it was intended to measure a pressure gradient of the same

order of magnitude for each of the four cores. Therefore the selected total superficial velocity at which each experiment was conducted was not the same in each case. The total superficial velocity values for the core in the section under study (“ $dP_2$ ” in Fig. 1) are reported in the caption of Fig. 2. Fig. 2a shows that apparent viscosity in the core-flood of Bentheimer sandstone increases in the low quality regime almost linearly up to the transition foam quality, which is observed at about  $f_g^* = 0.93$ . The proportional increase in apparent viscosity suggests that foam behaviour is nearly Newtonian. The high quality regime data plot almost on a straight line, which suggests Newtonian behaviour in the high quality regime as well. Berea sandstone (Fig. 2b) exhibited shear thinning behaviour in the low quality regime as indicated by the curvature in the trend of apparent viscosity on the plot as foam quality increases. The transition foam quality is observed at about  $f_g^* = 0.80$ . The transition appears less sharp compared to the case of Bentheimer. This, might however reflect the foam quality values at which apparent viscosity was measured, or the different density of data points.

Foam behaviour in the case of Sister Berea (Fig. 2c) is strongly shear thinning in the low quality regime. The transition foam quality in the experimental data is around  $f_g^* = 0.85$ . The high quality regime data plot on a straight line, similar to the case of Bentheimer, suggesting Newtonian behaviour in this regime. Data measured for Bandera Gray (Fig. 2d) appear to be of poorer quality: there is more scatter and the two regimes are not as distinct as for the other three cores. This could be due to greater pore irregularities in this low permeability sandstone, which could influence foam flow. The transition foam quality (maximum in apparent viscosity) is about  $f_g^* = 0.30$ . The behaviour of foam appears to be Newtonian in the low quality regime, though one could argue that the number of data points are not able to give a clear indication, or that the peak is an outlier measurement. In a scan of foam qualities at fixed total superficial velocity, gas superficial velocity is proportional to foam quality. Non-Newtonian behaviour of the gas manifests in a non-linear pressure gradient with respect to foam quality in the low-quality regime. Foam behaviour in the high-quality regime

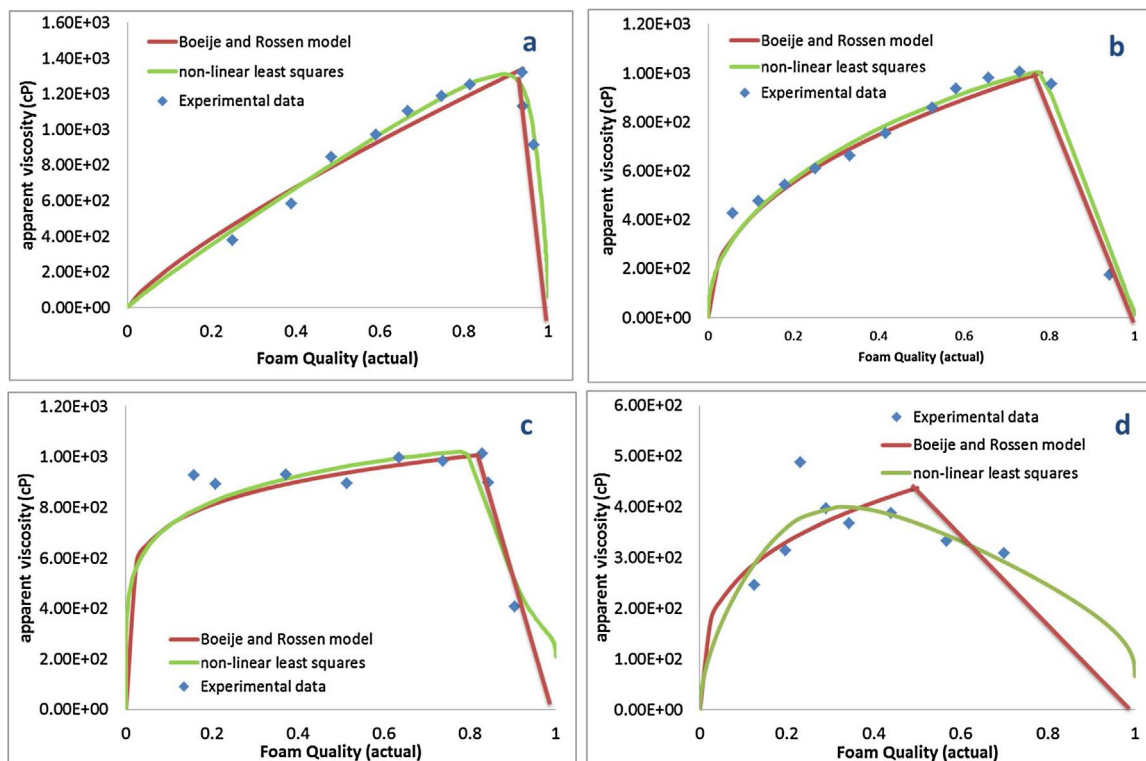


Fig. 2. Experimental data for foam scans of four sandstone cores: (a) Bentheimer, 1900 mD,  $u_t = 4.24$  ft/day (b) Berea, 90 mD,  $u_t = 0.671$  ft/day, (c) Sister Berea, 160 mD,  $u_t = 0.769$  ft/day, (d) Bandera Gray, 6 mD,  $u_t = 0.0716$  ft/day. Model fits are for the methods of Boeije and Rossen [34,46] and Eftekhari et al. [35]. The uncertainty of the experimental data (blue diamonds) is  $\pm 0.2$  bar, which is smaller than the marker.

**Table 2**

Foam-model parameters obtained by fitting the models of Boeije and Rossen [34,46] and Eftekhari et al. [35] to the foam-scans of the four sandstone cores.

Sandstone/Method/Parameter	Bentheimer (1900 mD)		Berea (90 mD)		Sister Berea (160 mD)		Bandera (6 mD)	
	Boeije & Rossen	Eftekhari et al.	Boeije & Rossen	Eftekhari et al.	Boeije & Rossen	Eftekhari et al.	Boeije & Rossen	Eftekhari et al.
<i>fmmob</i>	1.20E + 05	4.77E + 04	2.77E + 06	8.69E + 05	3.09E + 04	3.07E + 04	1.79E + 05	6.82E + 04
<i>epdry</i>	“high”	4.00E + 02	“high”	1.96E + 04	“high”	8.89E + 03	“high”	1.52E + 02
<i>fmdry</i>	2.74E – 01	2.71E – 01	3.36E – 01	3.36E – 01	3.91E – 01	3.96E – 01	5.31E – 01	5.49E – 01
<i>fmcap</i>	9.35E – 06	9.35E – 06	9.87E – 06	9.87E – 06	8.97E – 05	8.97E – 05	1.57E – 06	1.57E – 06
<i>epcap</i>	2.49E – 01	1.00E – 02	1.29E + 00	9.23E – 01	5.49E + 00	4.39E + 00	2.30E + 00	4.42E – 01

(above  $f_g^* = 0.85$ ) appears to be shear thinning with respect to gas velocity.

### 3.2. Modelling

The experimental data are fitted with the models of Boeije and Rossen [34,46] and with the non-linear least square fitting approach of Eftekhari et al. [35]. The two model's predictions are in good agreement with each other when fitting the foam-scan data obtained for the Bentheimer, Berea and Sister Berea cores. These three plots are discussed first. Table 2 provides a comparison between the parameters obtained with the two methods. The transition between the two regimes is by definition abrupt in the method of Boeije and Rossen [34,46]. This assumes a large value of *epdry*, e.g. greater than 10,000 (see Table 2). In the method of Eftekhari et al. [35] the value of this parameter is adjustable. With the latter method the transition as fitted is still relatively abrupt in the case of Berea and Sister Berea, while it is more gradual for Bentheimer. The modelled values of *fmdry* are in close agreement between the two methods. Thus by extension the modelled transition foam quality is also nearly the same in the two parameter fits. Parameter *fmmob* is the same for the fit to Sister Berea foam data but its value is about three times as large in the case of Boeije and Rossen [34,46] for Bentheimer and Berea. This can be explained by the parameter interaction which exists between *fmmob*, *fmcap* and *epcap*. The method of Boeije and Rossen interprets the foam scan as more shear-thinning. Thus it calculates a larger value of *epcap*. To compensate, the value of *fmmob* needs to be larger. Thus, it can be stated that the value of *fmmob* in the model fit is misleading. Since *fmcap* does not constitute a foam parameter per se, its value was kept constant between the two methods (Table 2), equal to the value calculated with the method of Eftekhari et al. [35]. Finally, neither of the two models can adequately describe the foam scan data for Bandera Gray. The method of Eftekhari et al. [35] appears to perform better due to its ability to assign a less-abrupt transition. Yet, neither model fit could be considered adequate. A trend of increasing limiting water saturation in the high quality regime, *fmdry*, is observed as permeability increases in all data. This results in a reduction in transition foam quality as permeability decreases.

Figs. 3 presents a prediction of the two regimes under variable gas and liquid velocities using the foam-model parameters of Eftekhari et al. [35] and Boeije and Rossen [34,46] (Table 2). The pressure gradient range for which contours are plotted was carefully selected to match the experimentally observed pressure gradients. The method of Boeije and Rossen [34,46] (dashed lines) shows that the transition between the two regimes is gradual in the case of Bentheimer and Bandera Gray, while it is abrupt for Berea and Sister Berea. For Berea and Sister Berea the behaviour is shear-thinning in the low quality regime. This phenomenon is reflected in the diverging pressure-gradient contours as gas velocity increases. The transition is more abrupt for both Bentheimer and Bandera Gray (*epdry* was set to a large value (20,000) which is an inherent assumption of the method of Boeije and Rossen [34,46]. This has a significant effect on the pressure gradient predictions, particularly near the transition between the two regimes.

As was suggested above, a reduction in critical foam quality as permeability decreases was observed (Fig. 2). Fig. 3, however, show

that the critical foam quality is velocity-dependent when foam is shear-thinning (Fig. 3b and c): critical foam quality shifts to higher values as velocity (and pressure gradient) increases.

Fig. 4, similar to Fig. 3, presents pressure-gradient plots obtained with the methods of Eftekhari et al. [35] and Boeije and Rossen [34,46]. However, in this case, the plots are computed for lower pressure gradients and a lower velocity range than observed in our experiments. This suggests a certain degree of extrapolation which makes predictions between the two models deviate further. This becomes more apparent in the cases of Bentheimer and Bandera where one model assumes an abrupt transition and the other a less-abrupt transition. Thus, similar to Fig. 3, the largest differences appear in the near the transition quality between regimes. However, even in the case where both models agree on the abruptness of transition (i.e. Berea, Fig. 4b and Sister Berea, Fig. 4c), differences in gas and liquid velocities are observed in the vertical and horizontal regions of the contours. The differences are up to 50%.

Fig. 4 reflects low capillary numbers, which can partly explain the observed differences. As a result, function  $F_5$  obtains in some cases a value greater than 1 (see discussion in Methods section), particularly when *epcap* is large (Sister Berea). This was not the case for plots in Fig. 3, where the calculated value of function  $F_5$  is always between 0 and 1. Table 3 shows the values of function  $F_5$  for both fitting methods. As the pressure gradient increases,  $F_5$  is closer to or less than 1. The cap that STARS applies on the function  $F_5$  is of practical importance: we deem that larger values could also be acceptable. Results for the method of Boeije and Rossen [34,46] follow the same trend. One could set different values of *fmcap* which would alter the value of *fmmob*. This was not done in this case for two reasons: (a) STARS suggests a maximum allowable value of *fmmob* = 100,000 [43] and (b) we wanted to highlight the effect of extrapolation of behaviour to a range of conditions very different from those of the experiment. Similarly,  $F_5$  could be constrained to values below 1 by choosing to plot  $\nabla p$  contours for even higher pressure gradients. The product of *fmmob*  $\times$   $F_5$ , shown in Table 3, is useful to compare the predicted mobility reduction by the two methods. It is this product that controls the predicted pressure gradient in the low-quality regime, rather than *fmmob* or  $F_5$  alone. There is no consistent trend in the product *fmmob*  $\times$   $F_5$  with permeability in Table 3, but if anything this product increases with decreasing permeability. This suggests that foam-flow resistance in the low-quality regime increases as permeability decreases. In other words, foam in the low-quality regime would not divert flow from low- to high-permeability layers.

### 3.3. Foam diversion calculations

We carry out diversion calculations using the foam-model parameter set obtained with the method of Eftekhari et al. [35] for three of the four sandstones used in this study. We do not make use of the foam-model parameters for Sister Berea because, as shown, the  $F_5$  function becomes strongly non-linear in the pressure range we model. These diversion calculations make predictions under steady-state conditions near the well with co-injection of gas and surfactant solution at a fixed injection pressure.

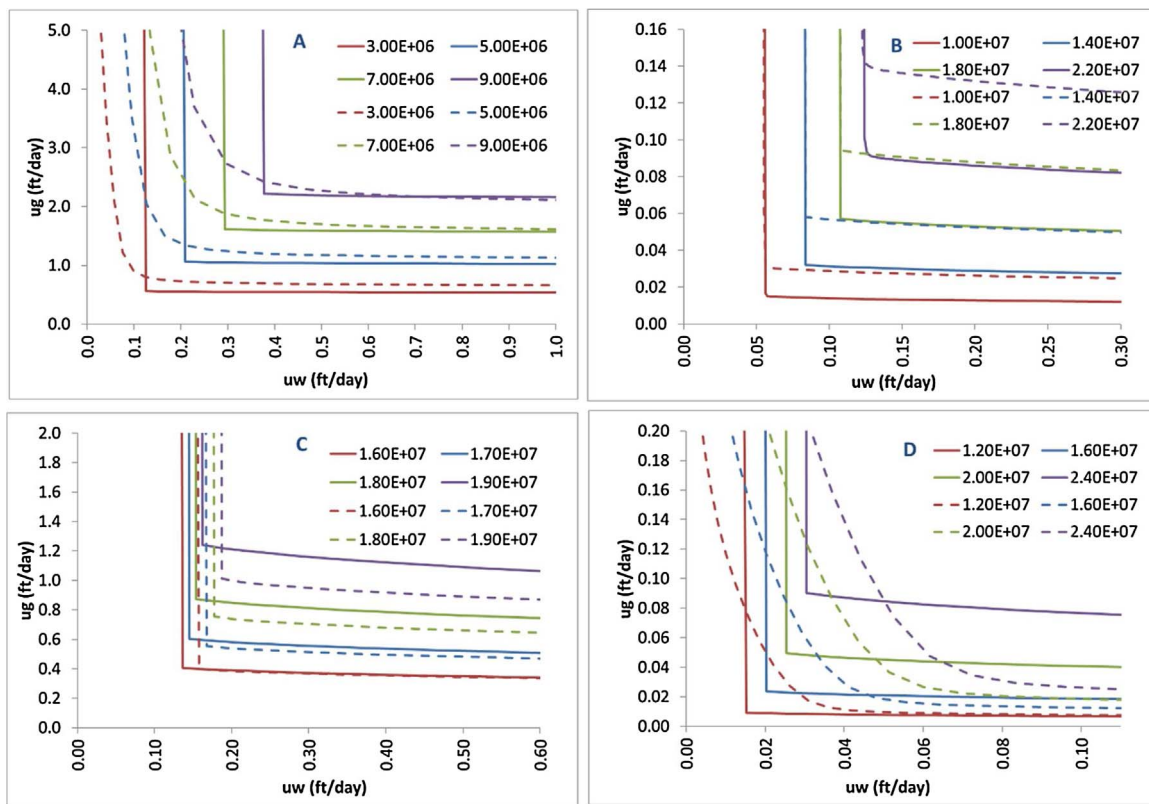


Fig. 3. Pressure gradient (Pa/m) as a function of superficial velocities of water and gas (ft/day), based on the foam model parameters of Table 2 obtained with the method of [35] and Boeje and Rossen (2015a) in continuous and dashed lines, respectively: (a) Bentheimer, (b) Berea, (c) Sister Berea, (d) Bandera Gray. Contours represent pressure gradient in Pa/m.

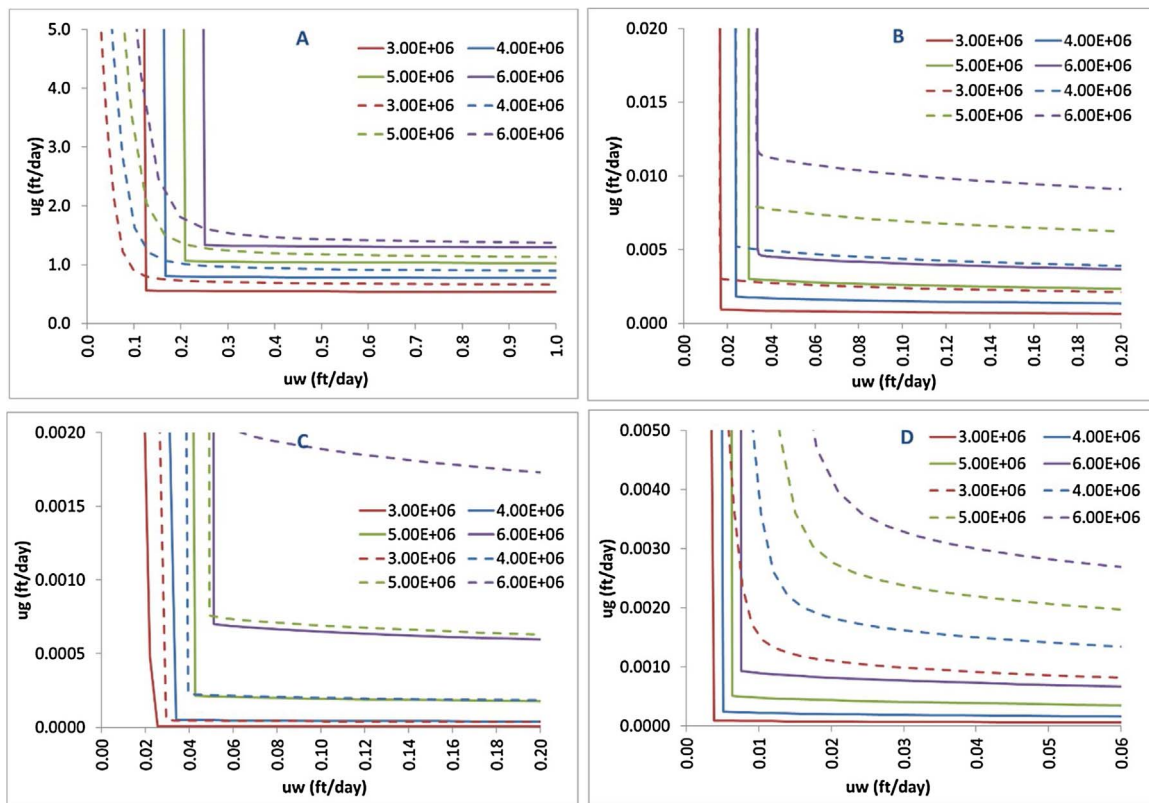
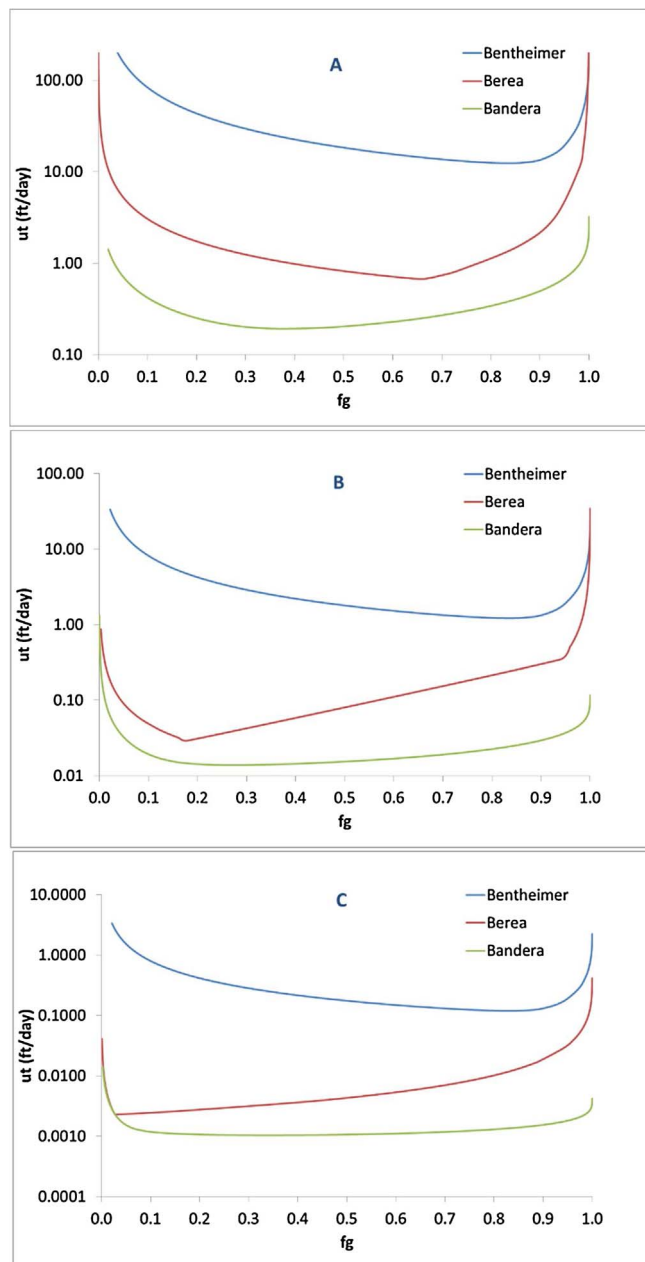


Fig. 4. Pressure gradient (Pa/m) as a function of superficial velocities of water and gas (ft/day), based on the foam model parameters of Table 2 obtained with the method of [35] and Boeje and Rossen (2015a) in continuous and dashed lines, respectively: (a) Bentheimer, (b) Berea, (c) Sister Berea, (d) Bandera Gray. Contours represent pressure gradient in Pa/m.

**Table 3**  
Values for function  $F_5$  and the product ( $fmmob \times F_5$ ) at different pressure gradients for the methods of Boeije and Rossen [34,46] and Eftekhari et al. [35].

Core		30 bar/m		40 bar/m		50 bar/m		60 bar/m	
		Boeije & Rossen	Eftekhari et al.						
Bentheimer	$F_5$	0.46	0.97	0.43	0.97	0.41	0.96	0.39	0.96
Berea		1.03	1.02	0.71	0.78	0.53	0.64	0.42	0.54
Sister Berea		8819.89	1429.33	1818.00	404.25	534.06	151.78	196.30	68.17
Bandera Grey		7.80	1.48	4.02	1.31	2.41	1.18	1.58	1.09
Bentheimer	$fmmob \times F_5$	5.57E + 04	4.62E + 04	5.18E + 04	4.61E + 04	4.90E + 04	4.60E + 04	4.69E + 04	4.59E + 04
Berea		2.85E + 06	8.88E + 05	1.97E + 06	6.81E + 05	1.47E + 06	5.54E + 05	1.16E + 06	4.68E + 05
Sister Berea		2.73E + 08	4.39E + 07	5.62E + 07	1.24E + 07	1.65E + 07	4.66E + 06	6.07E + 06	2.09E + 06
Bandera Grey		1.40E + 06	1.01E + 05	7.21E + 05	8.91E + 04	4.31E + 05	8.08E + 04	2.84E + 05	7.45E + 04



**Fig. 5.** Total velocity vs. foam quality plots for Bentheimer, Berea and Bandera Gray for pressure gradients of (a) 400 bar/m, (b) 40 bar/m and (c) 4 bar/m. The near-discontinuity in velocity over the range of foam quality observed for Berea is due to the abrupt transition at a given saturation. Note the y-axis is in logarithmic scale, to facilitate comparisons in velocity-value ratios between different layers.

Fig. 5 shows the total superficial velocity that foam would attain in each of the three layers if co-injected at a range of foam qualities, for three different pressure gradients: 400 bar/m, 40 bar/m, 4 bar/m. The layers are considered non-communicating. The first scenario of 400 bar/m pressure gradient is of course unrealistic and is only explored to illustrate the effect of foam-model parameters on diversion at higher pressure gradient.

In all cases (highest through to lowest pressure gradient) foam flows at a much larger velocity through the Bentheimer layer. This is observed at any foam quality, though the degree of diversion varies with injected foam quality. For instance, as foam reaches its strongest condition at a foam quality of approximately 95% (as shown in Fig. 2), the observed reduction in flow velocity is the greatest around this value of foam quality. This would allow flow to be directed to the other two layers; of course, the diversion in this case would only be relative since flow would still predominantly take place in the highest-permeability layer, namely Bentheimer. Table 4 reports the permeability ratios between Bentheimer and Berea, 21, and between Bentheimer and Bandera Gray, 317. Table 4 also presents a comparison of velocity ratios calculated using the model values of Fig. 5. If the velocity ratio between a set of two layers is lower than the respective permeability ratio, then this indicates potential for diversion. For instance, at a foam quality of 90% and a pressure gradient of 4 bar/m, one can expect diversion to both Berea (velocity ratio of 15 vs. permeability ratio of 21) and Bandera Gray layers (velocity ratio of 200 vs. permeability ratio of 317). The diversion takes place mostly to the mid-permeability sandstone, as one would expect.

As can be noted in Table 4 and Fig. 5, the behaviour can be different for different foam qualities or different pressure gradients. The lower the foam quality, the less efficient diversion is. In an extreme case, e.g. foam quality of 30% and pressure gradient 4 bar/m, the velocity ratio is higher than the permeability ratio between Bentheimer and Berea (velocity ratio of 125 vs. permeability ratio of 21). As pointed out above, the value of  $F_5$  can have a significant contribution in the predicted pressure gradients, and by extension the velocity values and ratios. Capping the value of function  $F_5$  would have affected the diversion calculations.

#### 4. Discussion

Considering the potential advantages of the application of foam EOR in heterogeneous media, this study presents an analysis of the effect of permeability on foam behaviour. Results show that permeability can have a significant impact on the critical foam saturation (higher- $k$  layer exhibiting lowest  $S_w^c$ ), which in turn influences the critical foam quality at which foam changes strong-state regime. When foam is shear-thinning the critical foam quality can shift to higher values at greater velocity (and pressure drop). Moreover, the experimental data show that the transition between the two regimes can be either abrupt or more gradual; however, no correlation was found between transition abruptness and permeability.

**Table 4**

Permeability and velocity ratios for Bentheimer, Berea and Bandera Gray, used for the diversion calculations of Fig. 5. The velocity ratios are calculated at 3 different foam qualities (30%, 60%, 90%). Values reported as "N/A" suggest that they could not be calculated analytically nor inferred from the plots in Figure 7.

Ratio/Foam Quality	Perm ratio (–)	Velocity ratios (–)								
		Ki/Kj	400 bar/m at quality (%):			40 bar/m at quality (%):			4 bar/m at quality (%):	
	–		30%	60%	90%	30%	60%	90%	30%	60%
Bentheimer	1	1	1	1	1	1	1	1	1	1
Bentheimer/Berea	21	N/A	N/A	5	34	8	4	91	31	7
Bentheimer/Bandera	317	1274	553	28	198	95	43	260	132	86

In modelling foam, current foam models make use of parameters that cannot be defined uniquely from constant-velocity foam-scan experiments. This was shown here by using two previously established techniques, namely those of Boeije and Rossen [34,46] and Eftekhari et al. [35]. The same foam-scan data can be fitted roughly equally well but the models yield different parameters. When one aims to predict pressure drops with the two different estimated parameter sets, large differences occur near the transition foam quality. Given the differences in the inferred extent of shear-thinning in the low-quality regime, the models extrapolate to very-different behaviour at pressure gradients much lower than those in the experiments.

When the foam-model parameters  $f_{mcap}$  and  $e_{pcap}$  are estimated, they should be carefully constrained to a range which is meaningful for the simulations to follow (i.e. the field study). This choice obviously affects the value of  $f_{mob}$ , since the parameters are correlated. In this study experiments were not carried out at field pressure gradients. As a result, the foam model extrapolates in a strongly non-linear fashion. This can potentially introduce differences between extrapolations between different model fits. Thus, it becomes apparent that a closer integration is required between the experimental foam study and simulation work. It is, therefore, recommended to perform foam core-floods under conditions similar to those to be applied in the field. Some degree of extrapolation is unavoidable since foam travelling in the reservoir experiences a range of different velocities, pressure gradients and saturations.

The foam-model parameters obtained by fitting the experimental data were used to predict foam diversion in a simplified situation where the layers do not communicate. The analysis shows that for the steady-state conditions studied, foam could partially divert flow to the low-permeability layers under certain foam-quality and pressure-gradient conditions. In these cases, superficial velocity was still significantly higher in the most-permeable layer. Based on this finding, one could expect that during the dynamic stage of foam co-injection (before steady-state is reached), foam would preferentially flow through the most permeable zones which would cause flow diversion to the low-permeable layers. This effect would, of course, be of limited duration since the pressure in these layers will increase.

The control of appropriate injection conditions is critical as the diversion effect varied for different foam qualities and pressure gradients; it was shown that under certain conditions it is possible that flow in the low permeability layer can be further inhibited by the application of foam.

## Acknowledgements

We gratefully acknowledge Shell Global Solutions International B. V. and PETRONAS for granting the permission to publish this work. We also thank the technical support of Michiel Slob at the Laboratory Geoscience & Engineering of TU Delft.

## References

- [1] L.L. Schramm, Foams: fundamentals and applications in the petroleum industry,

- Adv. Chem. Am. Chem. Soc. 242 (1994), <http://dx.doi.org/10.1021/ba-1994-0242>.
- [2] W.R. Rossen, Foam in Enhanced Oil Recovery. in R.K. Prud'homme and S.Khan "Foams: Theory, Measurements and Applications", Marcel Dekker, New York, 1996, pp. 413–464.
- [3] K. Mannhardt, L.L. Schramm, J.J. Novosad, Effect of Rock Type and Brine Composition on Adsorption of Two Foam-Forming Surfactants, (1993).
- [4] Y. Liu, R.B. Grigg, B. Bai, Salinity, pH, and Surfactant Concentration Effects on CO<sub>2</sub>-Foam, Society of Petroleum Engineers, 2005 SPE-93095.
- [5] R. Farajzadeh, R.M. Muruganathan, R. Krastev, W.R. Rossen, Effect Of Gas Type On Foam Film Permeability And Its Implications For Foam Flow In Porous Media, Society of Petroleum Engineers, 2010 SPE-131297.
- [6] A.D. Nikolov, D.T. Wasan, D.W. Huang, D.A. Edwards, The Effect of Oil on Foam Stability: Mechanisms and Implications for Oil Displacement by Foam in Porous Media, Society of Petroleum Engineers, 1986 SPE-15443.
- [7] H.C. Lau, Oapos Brien, Effects of Spreading and Nonspreading Oils on Foam Propagation Through Porous Media, (1988).
- [8] M.I. Kuhlman, Visualizing the Effect of Light Oil on CO<sub>2</sub> Foams, (1990).
- [9] M. Simjoo, M.N. Mahmoodi, P.L.J. Zitha, Effect of Oil Saturation on Foam for Acid Diversion, Society of Petroleum Engineers, 2009 SPE-122152.
- [10] M. Simjoo, P.L.J. Zitha, Effects of Oil on Foam Generation and Propagation in Porous Media, Society of Petroleum Engineers, 2013 SPE-165271.
- [11] M. Chabert, L. Nabzar, V. Beunat, E. Lacombe, A. Cuenca, Impact of Surfactant Structure and Oil Saturation on the Behavior of Dense CO<sub>2</sub> Foams in Porous Media, Society of Petroleum Engineers, 2014 SPE-169116.
- [12] L. Kapetas, S. Vincent-Bonnieu, R. Farajzadeh, A.A. Eftekhari, S.R. Mohd-Shafian, R.Z. Kamarul Bahrim, W.R. Rossen, Effect of permeability on foam-model parameters - an integrated approach from coreflood experiments through to foam diversion calculations, IOR 2015-18th European Symposium on Improved Oil Recovery (2015), <http://dx.doi.org/10.3997/2214-4609.201412124>.
- [13] L. Kapetas, et al., Effect of temperature on foam flow in porous media, 19th MEOS Conference, Bahrain, 2015 SPE 172820.
- [14] T.W. Patzek, Description of foam flow in porous media by the population balance method, surfactant-based mobility control, ACS Symp. Ser. Am. Chem. Soc. (1988) 326–341.
- [15] A.H. Falls, et al., Development of a mechanistic foam simulator: the population balance and generation by snap-off, SPE Reserv. Eng. 3 (3) (1988) 884–892.
- [16] A.R. Kovscek, T.W. Patzek, C.J. Radke, A mechanistic population balance model for transient and steady-state foam flow in Boise sandstone, Chem. Eng. Sci. 50 (23) (1995) 3783–3799.
- [17] H.J. Bertin, Foam diversion modeling using a bubble-Population correlation, Paper SPE59366 Presented at the 2000 SPE/DOE Improved Oil Recovery Symposium, Tulsa, OK, April 3-5, 2000.
- [18] S.I. Kam, Q.P. Nguyen, Q. Li, W.R. Rossen, Dynamic simulations with an improved model for foam generation, SPE J. 12 (1) (2007) 35–48.
- [19] P.L.J. Zitha, A New Stochastic Bubble Population Model for Foam in Porous Media, SPE/DOE Symposium on Improved Oil Recovery, Society of Petroleum Engineers, Tulsa, Oklahoma, USA, 2006.
- [20] Q. Chen, M. Gerritsen, A.R. Kovscek, Modeling foam displacement with the local-Equilibrium approximation: theory and experimental verification, SPE J. 15 (1) (2010) 171–183.
- [21] R.A. Ettinger, C.J. Radke, Influence of texture on steady foam flow in berea sandstone, SPE Reserv. Eng. 7 (1) (1992) 83–90.
- [22] T.J. Myers, C.J. Radke, Transient foam displacement in the presence of residual oil: experiment and simulation using a population-balance model, Ind. Eng. Chem. Res. 39 (8) (2000) 2725–2741.
- [23] S.I. Kam, W.R. Rossen, A Model for Foam Generation in Homogeneous Media, (2003).
- [24] D.H.S. Law, An Optimization Study For A Steam-Foam Drive Process In The Bodo Reservoir, Petroleum Society of Canada, Alberta, Canada, 1989.
- [25] T.W. Patzek, N.A. Myhill, Simulation of the Bishop Steam Foam Pilot, Society of Petroleum Engineers, 1989.
- [26] A.W. Fisher, R.W.S. Foulser, S.G. Goodyear, Mathematical Modeling of Foam Flooding, Society of Petroleum Engineers, 1990.
- [27] M.R. Islam, S.M.F. Ali, Numerical Simulation of Foam Flow In Porous Media, (1990).
- [28] L. Cheng, A.B. Reme, D. Shan, D.A. Coombe, W.R. Rossen, Simulating foam processes at high and low foam qualities, SPE/DOE improved oil recovery symposium, Copyright 2000, Society of Petroleum Engineers Inc. Tulsa, Oklahoma. 3-5 April 2000, 2000 SPE-59287.
- [29] E. Ashoori, D. Marchesin, W.R. Rossen, Roles of transient and local equilibrium

- foam behavior in porous media: traveling wave, *Colloids Surf A: Physicochem. Eng. Asp.* 377 (1–3) (2011) 228–242.
- [30] E. Ashoori, D. Marchesin, W.R. Rossen, Dynamic foam behavior in the entrance region of a porous medium, *Colloids Surf. A: Physicochem. Eng. Aspects.* 377 (2011) 217–227.
- [31] E. Ashoori, D. Marchesin, W.R. Rossen, Multiple foam states and long-distance foam propagation in porous media, *SPE J.* 17 (2012) 1231–1245.
- [32] E. Ashoori, D. Marchesin, W.R. Rossen, Stability analysis of uniform equilibrium foam states for EOR processes, *Transp. Porous Media* 92 (2012) 573–595.
- [33] K. Ma, et al., Estimation of parameters for the simulation of foam flow through porous media. part 1: the dry-out effect, *Energy Fuels* 27 (5) (2013) 2363–2375.
- [34] C.S. Boeije, W.R. Rossen, Fitting foam-simulation-model parameters to data: I. co-injection of gas and liquid, *SPE Reserv. Eval. Eng.* 18 (2) (2015) 264–272.
- [35] A.A. Eftekhari, J. Roebroeks, R. Farajzadeh, Optimization of Foam Model Parameters, *TIPM*, 2015.
- [36] W.T. Osterloh, M.J. Jante Jr., Effects of gas and liquid velocity on steady-State foam flow at high temperature, *SPE/DOE Enhanced Oil Recovery Symposium*, Society of Petroleum Engineers Inc., Tulsa, Oklahoma. 22–24 April 1992, 1992 SPE-24179.
- [37] J.M. Alvarez, H.J. Rivas, W.R. Rossen, 3, Unified Model for Steady-State Foam Behavior at High and Low Foam Qualities vol. 6, (2001), pp. 325–333 SPE-74141.
- [38] L. Kapetas, W.A. van El, W.R. Rossen, Representing Slow Foam Dynamics in Laboratory Corefloods for Foam Enhanced Oil Recovery, Society of Petroleum Engineers, Tulsa, Oklahoma, 2014 2014/4/12. SPE-169059.
- [39] Schlumberger, *ECLIPSE\* Reservoir Simulation Software*, Version 2010.2, Technical Description, (2010).
- [40] R. Farajzadeh, A. Andrianov, R. Krastev, G.J. Hirasaki, W.R. Rossen, Foam-oil interaction in porous media: implications for foam assisted enhanced oil recovery, *Adv. Colloid Interface Sci.* 183–184 (2012) 1–13.
- [41] R.T. Jacobsen, R.B. Stewart, Thermodynamic properties of nitrogen including liquid and vapor phases from 63 K to 2000 K with pressures to 10,000 Bar, *Natl. Stand. Ref. Data Syst.* 2 (4) (1973) 757–922.
- [42] E.F. Johnson, D.P. Bossler, V.O. Naumann, Calculation of Relative Permeability from Displacement Experiments, Society of Petroleum Engineers, 1959 1959/1/1. SPE-1023-G.
- [43] Computer Modeling Group (Calgary, Alberta, Canada), *STARS User's Guide*, Version, (2015) See also *GEM User's Guide*, Version 2015.
- [44] Z.I. Khatib, G.J. Hirasaki, A.H. Falls, Effects of capillary pressure on coalescence and phase mobilities in foams flowing through porous media, *SPE Reserv. Eng.* 3 (1988) 919–926 SPE 15442-PA.
- [45] Z. Zhou, W.R. Rossen, Applying fractional-flow theory to foam processes at the limiting capillary pressure, *SPE Adv. Technol. Ser.* 3 (1) (1995) 154–162 SPE-24180.
- [46] W.R. Rossen, C.S. Boeije, Fitting foam-simulation-model parameters to data: II. surfactant-alternating-gas foam applications, *SPE Reser. Eval. Eng.* 18 (2) (2015) 273–283.
- [47] A.R. Kovscek, W.P. Tadeusz, C.J. Radke, Mechanistic foam flow simulation in heterogeneous and multidimensional porous media, *SPE* 2 (December) (1997) 511–526.